Dynamics of the intertropical convergence zone over the western Pacific during the Little Ice Age

Hong Yan [1,2*], Wei Wei [3], Willie Soon [4], Zhisheng An [1,2], Weijan Zhou [1,2], Zhonghui Liu [5], Yuhang Wang [1], and Robert M. Carter [6]

Accepted for publication in Nature Geoscience, 29 January 2015. Doi:10.1038/NGEO2375

Precipitation in low latitudes is primarily controlled by the position of the intertropical convergence zone, which migrates from south to north seasonally. The Little Ice Age (defined as AD 1400-1850) was associated with low solar irradiance and high atmospheric aerosol concentrations as a result of several large volcanic eruptions. The mean position of the intertropical convergence zone over the western Pacific has been proposed to have shifted southwards during this interval, which would lead to relatively dry Little Ice Age conditions in the northern extent of the intertropical convergence zone and wet conditions around its southern limit. However, here we present a synthesis of palaeo-hydrology records from the Asian-Australian monsoon area that documents a rainfall distribution that distinctly violates the expected pattern. Our synthesis instead documents a synchronous retreat of the East Asian Summer Monsoon and the Australian Summer Monsoon into the tropics during the Little Ice Age, a pattern supported by the results of our climate model simulation of tropical precipitation over the past millennium. We suggest that this pattern over the western Pacific is best explained by a contraction in the latitudinal range over which the intertropical convergence zone seasonally migrates during the Little Ice Age. We therefore propose that rather than a strict north-south migration, the intertropical convergence zone in this region may instead expand and contract over decadal to centennial timescales in response to external forcing.

Tropical rainfall varies in association with the seasonal migrations of the circum-global intertropical convergence zone (ITCZ) and the closely related monsoonal land-sea coupled systems. On millennial to orbital timescales, both paleoclimate proxy research and climate modelling have suggested that the precipitation in the tropical and subtropical monsoon areas varies in parallel with latitudinal migration of the ITCZ, being characterized by opposing variations in the two hemispheres[1-5]. With southward migration of the ITCZ, the precipitation in Northern Hemisphere summer monsoon area decreases while the precipitation in the Southern Hemisphere summer monsoon area increases; and vice versa. Climate models suggest that the millennial to orbital timescales migration of the mean annual position of the ITCZ is related to changes in Northern Hemisphere high-latitude climate, the Atlantic meridional overturning circulation and the asymmetrical insolation input between hemispheres[1-4,9]. A southward migration of the ITCZ occurs when the North Atlantic region is relatively cold due to enhanced high-latitude ice cover and a slowdown of the Atlantic meridional overturning circulation[1-3]. Conversely, a northward migration of the ITCZ mean position is usually driven by the increased Northern Hemisphere insolation input relative to the Southern Hemisphere[2,4,9].

The dynamical variation of the ITCZ rainbelt has also been considered the main factor for centennial timescale hydrologic changes in tropical areas over the last millennium[6,7]. A large body of paleo-proxy evidence suggests that during the relatively cold Little Ice Age period (LIA, ~AD 1400-1850), regions located at the northern limit of the ITCZ rainbelt, including the pan-Caribbean region[9,10], became drier relative to both the warm Medieval Climate Anomaly period (MCA, ~ AD 800-1300) and the most recent 150 years, pointing to a possible southward shift of the ITCZ[6,7]. Meanwhile, some hydrological records from the southern boundary of the ITCZ that reflect a wetter LIA are also evidence in supported of southward migration of the ITCZ mean position[6,11,12].

Although a similar/parallel southward migration of ITCZ has been described during the LIA in open ocean areas of the Pacific[7], the pattern of change for the west Pacific marine- continental ITCZ remains less well established[8]. In this study, we synthesized high-resolution paleo-hydrology records from the East Asian-Australian summer monsoon regions during the past millennium to test the variation pattern of the west Pacific ITCZ. Surprisingly, we found that the west Pacific region has yielded a precipitation distribution pattern in contradiction of what would normally be predicted from the southward shift of the ITCZ mean position during the LIA. Instead of the expected pattern, both the EASM and the ASM retreated synchronously during the LIA and the core precipitation zones converged more narrowly within the tropics.

Paleo-hydrology records from the EASM area

Many studies, including those utilizing speleothem records[2,13-16], lake sediment records[8,17-19] and historical documentary records[20], have focused on describing the hydrological changes in EASM area over the last millennium, with the results showing obvious regional differences (Fig. 1, Fig. s1 and s2). The paleo-hydrology records from the northern limit of the EASM, including a lake sediment record (D1)[18], a historical archive record (D2)[20] and two stalagmite records (D3 and D4)[13,14], show similar variations over the last millennium and indicate that this region was hard hit by droughts during LIA relative to MCA and the last 150 years (Fig.1, Fig. 3 and Fig. s1). Conversely, lake sediment records from the southern coast of China (W2 in Fig.1 and Fig. s2)[17,19] and the northern South China Sea (W3 in Fig.1 and Fig. s2)[8] display a clear wet condition during the LIA relative to the MCA and the last 150 years. At the same time, the hydrological records located between these two regions reveal a gradual transition from dry to wet. The speleothem record (D5 in Fig.1 and Fig. s1)[15] from central China reveals a moderate drought during the LIA while similar records (N1 and N2 in Fig.1 and Fig. s2)[2,16] from southwest China, located near the transitional zone, show no significant difference between the LIA and the MCA. The spatial differences from north to south across China point to a probable retreat of the EASM during the LIA. This retreat led to reduced northward transport of monsoon moisture, a contracted core zone of precipitation, a relatively dry condition near the modern northern limit of the EASM and more precipitation in southern China during the LIA.

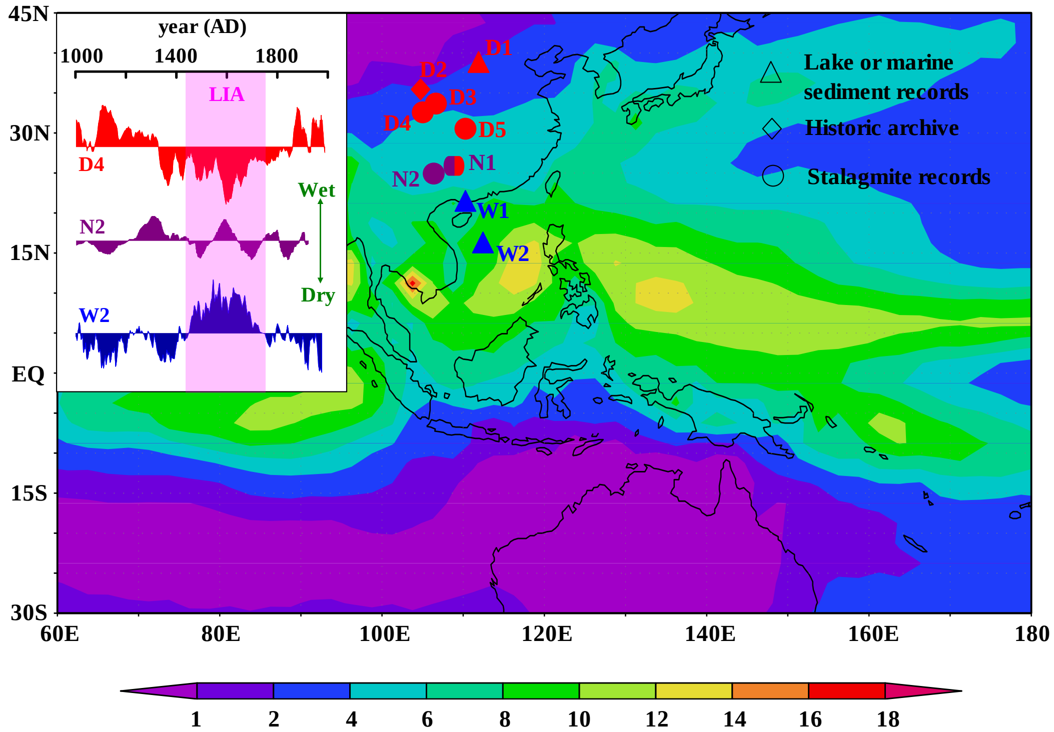

Figure 1 Pattern of rainfall within the EASM region during LIA. *The background contours show summer mean precipitation (from June to October, mm/day) in the EASM area as derived from NCEP reanalysis2 from January 1979 to December 2010. Locations of proxy-hydrology records in the EASM area are indicated: D1[18], D2[20], D3[13], D4[14], D5[15] N1[2], N2[16], W1[17,19] and W2[8]. Locations that were dry, without apparent change and wet during the LIA relative to the MCA/recent 150 years are marked in red, purple and blue, respectively. The three hydrologic conditions are objectively defined by the Relative Wet Index and t-test (see method for details).*

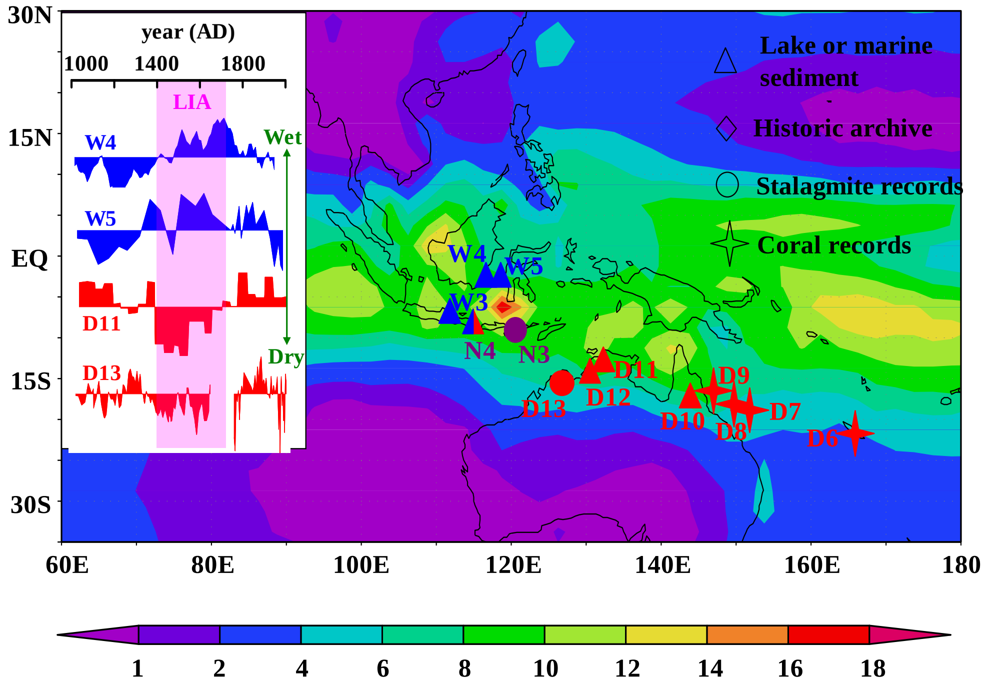

Figure 2 Pattern of rainfall within the ASM region during LIA. *The background contours show summer mean precipitation (from December to February, mm/day) in the ASM area derived from NCEP reanalysis2 from January 1979 to December 2010. Locations of proxy-hydrology records in the ASM area are also indicated: D6[25,26], D7[27], D8[24], D9[23], D10[28,29], D11[21], D12[21], D13[22], N3[31], N4[32], W3[30], W4[11] and W5[6,12]. Locations that were dry, without apparent change and wet during the LIA relative to the MCA/recent 150 years are marked in red, purple and blue, respectively.*

Paleo-hydrology records from the ASM area

Hydrological variations in the ASM area over the last millennium are less well established than those in the EASM area, but the retreat of the ASM during the LIA is still evident (Fig. 2, Fig s3, s4 and s5). The 1000-year long fluvial sedimentary records from the floodplain of Daly River (D11 in Fig.2) [21] and the Magela Creek Flood Plain (D12 in Fig. 2 and Fig. s3)[21] in the ‘Top End’ area of the Australia suggest a reduced river discharge and dry conditions in this region during the LIA. Meanwhile, a nearby speleothem record provides further confirmation of dry conditions in tropical northwestern Australia during AD 1400-1700 (D13 in Fig. 2 and Fig. s3)[22]. The more positive stalagmite $\delta^{18}O$ during the LIA relative to the MCA and the recent 150 years has been interpreted as indicating less precipitation in this region[22].

The multi-proxy records from northeastern Australia also indicate dry conditions during the LIA (Fig. s3 and Fig. s4). The northeast tropical Queensland river flow and rainfall reconstruction derived from Great Barrier Reef coral luminescence studies (D9)[23] clearly show less precipitation during the LIA than during the 20th century. Meanwhile, all three seawater $\delta^{18}O$ records derived from coral $\delta^{18}O$ and Sr/Ca in Great Barrier Reef (D8)[24], New Caledonia (D6)[25,26] and Flinders Reef (D7)[27] exhibit more positive values (consistent with dry conditions) during the LIA compared to the 20^{th} century. The dry LIA in northeastern tropical Australia has recently been further confirmed by two new peat humification records from Queensland (D10 in Fig. 2 and Fig. s3), which document clearly that dry conditions prevailed during the LIA[28,29]. These records, together with the fluvial sedimentary and speleothem records from tropical western Australia, indicate that dry conditions probably covered the whole tropical Australian continent during the LIA.

In contrast to the drier conditions in northern Australia, several paleo-hydrology records from the Indo-Pacific Warm Pool region, including the organic matter $\delta^{13}C$ record of lake sediment from Java (W3)[30], a leaf wax δD record from Makassar Strait (W4)[11] and the sea surface salinity record derived from $\delta^{18}O$ and Mg/Ca of planktonic foraminifera from Makassar Strait (W5)[6,12], consistently suggest more precipitation and wetter conditions during the LIA than that during the MCA/last 150 years (Fig. 2 and Fig. s5). However, some hydrological records from southern Indonesia, located between the Warm-pool and northern Australia, show no clear dry or wet conditions during the LIA[31-34]. For example, the stalagmite $\delta^{18}O$ record from southern Indonesia shows no apparent difference between the LIA and the MCA or most recent 150 years (N3 in Fig. 2 and Fig. s5)[31], while the δD of terrestrial plant wax indicates that rainfall has steadily increased in East Java over the last millennium (N4)[32].

The general pattern of increased precipitation (LIA relative to MCA/recent 150 years) from the northern Australia to Indo-Pacific warm pool area is similar to that observed in the EASM area, and also consistent with a weakened ASM during the LIA.

Empirical Explanation and Climate Modelling

The observed dry condition in the northern Australia monsoon area during the LIA argues against the established southward ITCZ migration hypothesis in the west Pacific region. It follows that the ITCZ migration theory, which was mainly proposed to explain millennial to orbital scale tropical hydrological changes[1-4,9], does not explain the documented decadal to centennial scale hydrological variations that occurred over the western Pacific region during the last millennium. Instead, we propose the alternative and more physically plausible hypothesis that a contraction of the ITCZ/monsoon zones during the LIA within the western Pacific, accompanied by a synchronized retreat of both the EASM and the ASM (Fig. s6 and Fig. s7).

Meanwhile, although the driving force of ITCZ migration on millennial to orbital timescale has been well described[1-4,9], the mechanism of the ITCZ dynamics on a decadal-centennial scale (e.g. the southward migration proposed for LIA[7]) remains unclear[7,8,35]. For example, a 5° southward ITCZ shift during LIA was proposed by one previous study[7], but the possible forcing factors for ITCZ migration, such as the freshwater forcing initiated around the North Atlantic Ocean and orbitally-driven asymmetrical insolation input between hemispheres (Fig. 3b, 3c), did not show marked changes during the LIA. In addition, a recent constraint suggests that a 5° southward shift would implicate a large cross-equatorial atmospheric heat transport of 1.7 PW and an inter-hemispheric tropical SST gradient (i.e., 0-20°N minus 0-20°S) of 1.5 to 3.7 K, yet neither of which has been detected[35].

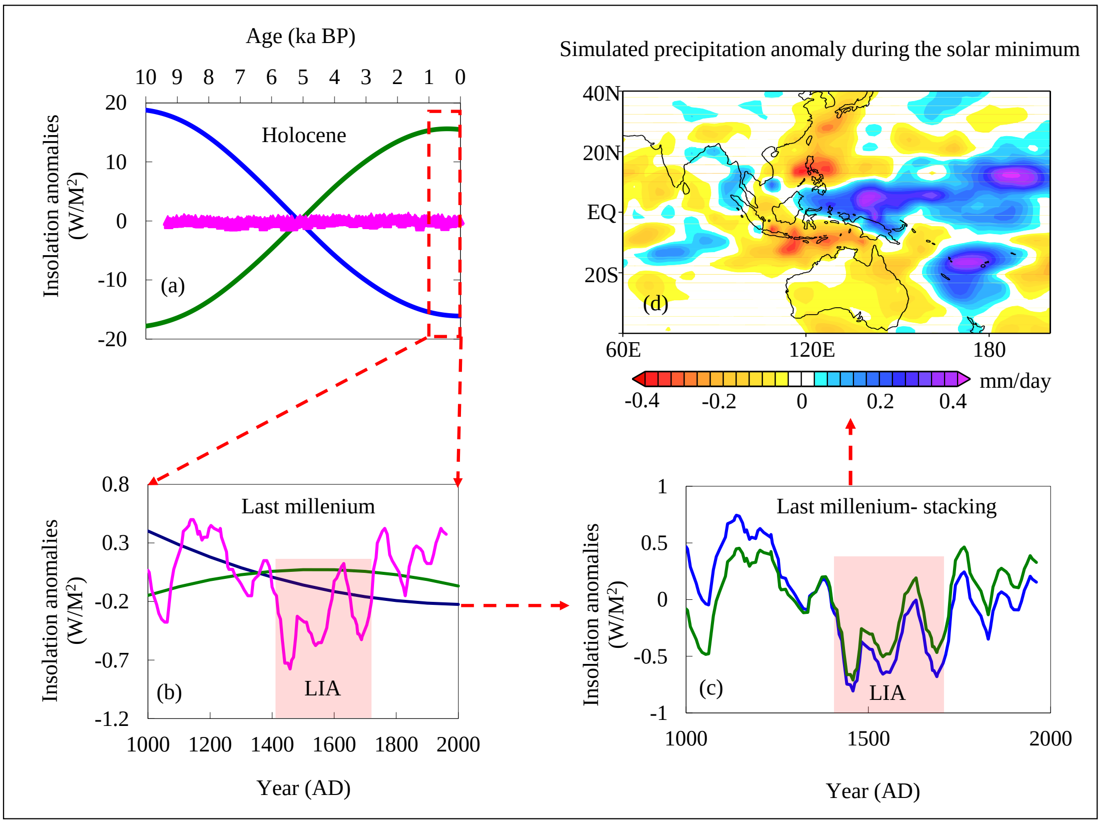

Figure 3 Forcing and modeling results. *Solar forcing representing the solar output (pink)[37,38] and orbital parameters (blue and green lines are the July and January insolation at 23.5°N and 23.5°S, respectively)[36] during the Holocene (a, orbital changes dominating) and past millennium (b, solar output dominating). (c): total solar forcing of the 23.5°N (blue) and the 23.5°S (green) has been calculated by adding up the changes of the solar output and orbital parameters. (d): The simulated annual mean precipitation anomaly during the late solar Maunder minimum phase (AD 1690-1740) of the LIA with reference to the long-term mean (AD 1000-1800) in a MPI-ESM last millennial simulation[42].*

Solar insolation on the earth depends not only on the orbital parameters[36] but also on the direct irradiance variations of the sun[37]. The precessional cycles of the equinoxes of Earth-Sun orbit have been demonstrated to be the most important orbital parameters that are linked with tropical hydrological changes. The precessional forcing has a non-linear impact on the insolation budget and usually produces opposite insolation variations, and anti-symmetric forcing, between the Northern and Southern Hemisphere (Fig. 3)[36], and thus changes the mean position of the global ITCZ through the inter-hemispheric insolation and thermal gradients that are established. In contrast to the precessional forcing, the intrinsic changes of solar irradiance are symmetrical and hence produce a synchronized forcing on both hemispheres[37]. On the orbital timescale, the amplitude of insolation change caused by fluctuations of the orbital precessional cycle is much larger than that induced by variations in solar output (Fig. 3a)[36,38]. For this reason, the ITCZ is expected to migrate north-south in phase with the changing inter-hemispheric insolation gradients. However, this situation reversed over the last millennium, during which period the insolation variation caused by orbital change became much smaller than that caused by fluctuations in direct solar irradiance (Fig. 3b and Fig. s8)[36,37]. The small variability of asymmetrical orbital insolation forcing during the last millennium seems too inadequate to cause large meridional migration of the ITCZ mean position during the LIA.

When adding the changes from both orbital parameters and solar irradiance, we have found that the insolation in the Northern and Southern Hemispheres shows a similar variation pattern over the last millennium, with a decreased insolation during the LIA relative to the MCA/ last 150 year intervals (Fig. 3c and Fig. s8). Such hemispherically symmetric forcing from intrinsic solar irradiance probably contributed to the synchronized retreats of both the EASM and the ASM during the LIA. On the other hand, large volcanic eruptions (i.e., especially frequent and persistent volcanic activity around the tropical western Pacific region[39]), may also yield symmetrical forcing between two hemispheres and could therefore also help to drive contractions of the monsoon/ITCZ belts. For example, some strong volcanic eruptions have been detected during the LIA (i.e., coinciding with the Maunder Minimum and Dalton Minimum)[39,40].

Our proposal of a contracted monsoon-ITCZ in the Western Pacific region is also supported by published investigations of global monsoon precipitation in response to natural and anthropogenic forcings in the last millennium, based upon simulations with the coupled ocean-atmosphere model ECHO-G[40]. The simulated results suggest a symmetrical decrease in monsoon precipitation in both hemispheres during the LIA (see ref[40] for details) with the three weakest periods around 1460, 1685, and 1800 (which respectively correspond to the deepest parts of the Spörer Minimum, Maunder Minimum, and Dalton Minimum intervals of reduced irradiance)[40], while the global monsoon strengthened nearly everywhere in the continental monsoon regions during the modeled MCA interval[40]. In addition, the simulated precipitation increases in tropical Indonesia and rainfall decreases in northern Australia during the solar minima were also demonstrated in a recent idealized solar sensitivity experiment using the coupled climate model CCSM3[41].

In order to analyze the impact of solar activity on tropical precipitation over the last millennium independently, we have also deployed the Coupled Model Intercomparison Project Phase 5 (CMIP5) style model from the Max Planck Institute Earth System Model (MPI-ESM) millennium simulation (see supplementary materials for details), using only solar variability as external forcing[42]. The model results (Fig. 3d), which show decreased precipitation in west Pacific subtropical monsoon area of both hemispheres and more rainfall in equatorial area during the periods of low solar activity, offer hints in support our proposal of a contracted monsoon/ITCZ in west Pacific during the LIA (Fig. 3d and Fig. s9).

The simulated reduced global monsoon precipitation during the LIA was primarily attributed to reduced solar irradiance by Liu et al (2009). Our own simulation independently confirmed this result (Fig. s9). Changes in the total amount of effective shortwave radiative forcing (i.e., including short-term pulses of forcing from globally influential volcanic eruptions) can reinforce the thermal contrast between the continent and ocean (Table 3 in ref[40]), thereby resulting in the centennial scale variations in the global monsoon strength[40]. Land has a much smaller heat capacity than ocean. When the effective radiative flux increases during the local summer, the land warming is much stronger than the warming of adjacent ocean and thus the thermal contrast between continent and ocean gets reinforced[40]. This increased thermal contrast further enhances the pressure differences between land monsoon regions and the surrounding oceans (Table 3 in ref[40]) and therefore strengthens the monsoon circulation and its associated rainfall[40]. A decrease in irradiance during the LIA, plus the unique land-sea distribution in the west Pacific region, would thus produce the decreased seasonal extremes of the monsoon moisture transport and the consequent contraction of the west Pacific monsoon/ITCZ.

It is worth noting that the model results also implied an increased zonal precipitation contrast between east and west tropical Pacific during the LIA (Fig. s9 and ref[40]), which would probably manifest itself as an enhanced Pacific Walker circulation. Although some temperature reconstructions proposed an El Nino-like SST pattern in tropical Pacific during the LIA[43,44], the hydrological studies, based upon either proxy records[8,11,12,45] or model simulations[46], present a clear strengthening of Pacific Walker circulation during the LIA, which should result in more precipitation in the Indo-Pacific warm-fresh pool region (see SI for further discussion). That is to say, the scenario of a contracted western Pacific monsoon/ITCZ and an enhanced Pacific Walker circulation probably co-existed during the LIA interval, with both mechanisms contributing extra precipitation to the warm pool region.

Our main findings highlight the difficulty of applying the conventional interpretation of ITCZ migration to explain the hydrological changes in the East Asian-Australian monsoon area that are known to have occurred during the last millennium. It remains the case, however, that the detailed position of the west Pacific monsoon/ITCZ during the LIA, the range of the ITCZ-monsoonal meridional contraction (locally or globally) and the mechanism of the contractions that have occurred are still not fully understood. Developing an enhanced understanding of this topic requires the collection of additional high-resolution paleo-hydrology proxy data, and the application of insightful and focused climate modeling studies.

Methods

Definition of the MCA and LIA

To investigate the hydrologic changes between the MCA and the LIA, we have defined these terms as represented by distinct three-century-long intervals. The medieval interval, which is usually defined from AD 800 to 1300 in previous studies[47], has here been defined from AD 1000 to 1300 because we mainly focused on the past millennium. Correspondingly, a three-century-long LIA has been defined from AD 1400 to 1700 based on the minimum of the solar activity[37]. The Welch's t-test result suggested a significant difference in solar irradiance forcing between AD 1400-1700 and AD 1000-1300.

Dry/wet conditions between LIA and MCA/recent 150 years

Proxy records from the Asia- western Pacific- Australia monsoon areas were selected to investigate the hydrological changes between the LIA and the MCA/recent 150 years based on three main criteria. First, the temporal resolution of the data is better than 50 years and sufficient to distinguish among the MCA- LIA- recent 150 years intervals. Second, the dating error of the record is less than 100 years. Third, the proxy record has been used to reflect precipitation/humidity/monsoon variation in the original reference. Both the Relative Wet Index (RWI) and t-test were used to define and compare the dry/wet conditions between the LIA and the MCA/recent 150 years. The RWI and t-test were performed as following:

RWI: The RWI between the LIA and the MCA for each proxy record was defined by calculating the RWI = (mean value during the LIA minus mean value during the MCA)/the standard deviation. This method is also used to calculate the RWI between the LIA and the most recent 150 years. The time spans of the four coral records were too short to calculate the RWI between the LIA and the MCA. Thus we only calculated the RWI between the LIA and the most recent 150 years, the RWI being modified as RWI = (mean value before AD 1850- mean value after AD 1850)/the standard deviation. Before the calculation, the resolution of each proxy record was adjusted to one year using linear interpolation. The calculated RWI values are given in Table s1.

t-test: The significance of the difference between the LIA and the MCA/recent 150 years for each hydrological series was evaluated by applying an unpaired Welch's t-test, which does not require equal variance. Before the calculation, the effective sample size of the t-test was adjusted following the method in Trenberth (1984)[48] and Bretherton et al (1999)[49] (see the next section, Correlation analysis, for details). The calculated p values are displayed in Table s1. A p value less than 0.05 is considered statistically significant. As seen in Table s1, among the significant differences ($p < 0.05$), only two p values are about 0.02 and the rest are < 0.01. Thus, our results are statistically of high significance.

If the RWI between the LIA and the MCA is greater than 50% and the p value of the t-test is less than 0.05, a wet LIA relative to the MCA is defined. If the RWI between the LIA and the MCA is less than -50% and the p value of the t-test is less than 0.05, then a dry LIA relative to the MCA is defined. If the p value of the t-test is more than 0.05 or the RWI between the LIA and the MCA is between - 50% and 50%, no apparent precipitation change is defined between the LIA and the MCA. This method was also used to define the dry/wet conditions between the LIA and the recent 150 years. Locations that were dry, had no apparent change or were wet during the LIA relative to the MCA/recent 150 years are coloured red, purple and blue in all map figures, respectively. If the dry/wet condition between the LIA and the MCA is different from the dry/wet condition between the LIA and the most recent 150 years, then a combined colour is used. For example, the record N1 has a no apparent change during the LIA relative to the MCA and a dry LIA relative to the most recent 150 years. Thus N1's label has purple left and red right.

Correlation analysis

For two time series, X and Y, Pearson correlation coefficient r_{xy} was calculated as

$$r_{xy} = \frac{\sum_{i=1}^{n}(x_i - \bar{x})(y_i - \bar{y})}{(n-1)s_x s_y}$$

Where n is the sample number, $\bar{x}$ and $\bar{y}$ are the sample means of *X* and *Y*, and S_x and S_y are the sample standard deviation of *X* and *Y*. For two time series (X and Y) with smoothing, we have to consider and adjust the autocorrelation in X and Y by using effective sample size or effective number of independence values. Following Trenberth (1984)[48] and Bretherton et al (1999)[49], we first calculated τ , the time between independent values (or the time to obtain a new degree of freedom) according to the following equation[50]:

$$\tau = 1 + 2\sum_{l=1}^{(n-1)} r_{xl} r_{yl}$$

Where r_{xl} and r_{yl} are the autocorrelation at lag l for X and Y. The effective number of independence values was calculated as $n_{eff} = n/\tau$, and the student t-value for assessing significance was calculated as

$$t = \frac{r_{xy}\sqrt{n_{eff} - 2}}{\sqrt{(1 - r_{xy}^2)}}$$

Competing financial interests

The authors declare no competing financial interests

References

1 Chiang, J. C. & Bitz, C. M. Influence of high latitude ice cover on the marine Intertropical Convergence Zone. *Climate Dynamics* **25**, 477-496 (2005).

2 Wang, Y. J. *et al.* The Holocene Asian monsoon: Links to solar changes and North Atlantic climate. *Science* **308**, 854-857 (2005).

3 Zhang, R. & Delworth, T. L. Simulated tropical response to a substantial weakening of the Atlantic thermohaline circulation. *Journal of Climate* **18**, 1853-1860 (2005).

4 Timmermann, A., Lorenz, S., An, S., Clement, A. & Xie, S. The effect of orbital forcing on the mean climate and variability of the tropical Pacific. *Journal of Climate* **20**, 4147-4159 (2007).

5 Schneider, T., Bischoff, T. & Haug, G. H. Migrations and dynamics of the intertropical convergence zone. *Nature* **513**, 45-53 (2014).

6 Newton, A., Thunell, R. & Stott, L. Climate and hydrographic variability in the Indo-Pacific Warm Pool during the last millennium. *Geophysical Research Letters* **33**, L19710 (2006).

7 Sachs, J. P. *et al.* Southward movement of the Pacific intertropical convergence zone AD

1400-1850. *Nature Geosci* **2**, 519-525 (2009).

8 Yan, H. *et al.* South China Sea hydrological changes and Pacific Walker Circulation variations over the last millennium. *Nature Communications* **2**, 293 (2011).

9 Haug, G., Hughen, K., Sigman, D., Peterson, L. & Rohl, U. Southward migration of the Intertropical Convergence Zone through the Holocene. *Science* **293**, 1304 (2001).

10 Hodell, D. A. *et al.* Climate change on the Yucatan Peninsula during the little ice age. *Quaternary Res* **63**, 109-121 (2005).

11 Tierney, J., Oppo, D., Rosenthal, Y., Russell, J. & Linsley, B. Coordinated hydrological regimes in the Indo-Pacific region during the past two millennia. *Paleoceanography* **25**, PA1102 (2010).

12 Oppo, D. W., Rosenthal, Y. & Linsley, B. K. 2,000-year-long temperature and hydrology reconstructions from the Indo-Pacific warm pool. *Nature* **460**, 1113-1116 (2009).

13 Tan, L. *et al.* Centennial-to decadal-scale monsoon precipitation variability in the semi-humid region, northern China during the last 1860 years: Records from stalagmites in Huangye Cave. *The Holocene* **21**, 287-296 (2010).

14 Zhang, P. Z. *et al.* A Test of Climate, Sun, and Culture Relationships from an 1810-Year Chinese Cave Record. *Science* **322**, 940-942 (2008).

15 Hu, C. *et al.* Quantification of Holocene Asian monsoon rainfall from spatially separated cave records. *Earth and Planetary Science Letters* **266**, 221-232 (2008).

16 Qin, J. *et al.* High resolution stalagmite records of climate change since 800 AD in Libo, Guizhou. *Carsologica Sinica* **27**, 266-272 (In Chinese with English abstract) (2008).

17 Chu, G. *et al.* The ‘mediaeval warm period’drought recorded in Lake Huguangyan, tropical South China. *The Holocene* **12**, 511-516 (2002).

18 Liu, J. B. *et al.* Humid medieval warm period recorded by magnetic characteristics of sediments from Gonghai Lake, Shanxi, North China. *Chinese Science Bulletin* **56**, 2464-2474 (2011).

19 Zeng, Y. *et al.* The wet little Ice age recorded by sediments in Huguangyan Lake, tropical South China. *Quaternary International* **263**, 55-62 (2011).

20 Tan, L. C., Cai, Y. J., Yi, L., An, Z. S. & Ai, L. Precipitation variations of Longxi, northeast margin of Tibetan Plateau since AD 960 and their relationship with solar activity. *Clim Past* **4**, 19-28 (2008).

21 Wasson, R., Bayliss, P. & Clelland, S. River flow and climate in the 'top end' of Australia for the last 1000 years, and the Asian-Australian monsoon. In Kakadu National Park Landscape Symposia Series 2007-2009. Symposium 4: Climate change. ed S Winderlich, 6-7 August 2008, Gagudju Crocodile Holiday Inn Kakadu National Park. Internal Report 567, January, Supervising Scientist, Darwin, 15-31. (2010).

22 Denniston, R. F. *et al.* A Stalagmite record of Holocene Indonesian-Australian summer monsoon variability from the Australian tropics. *Quaternary Science Reviews* **78**, 155-168 (2013).

23 Lough, J. M. Great Barrier Reef coral luminescence reveals rainfall variability over northeastern Australia since the 17th century. *Paleoceanography* **26**, PA2201 (2011).

24 Hendy, E. *et al.* Abrupt decrease in tropical Pacific sea surface salinity at end of Little Ice Age. *Science* **295**, 1511-1514 (2002).

25 DeLong, K. L., Quinn, T. M., Taylor, F. W., Shen, C.-C. & Lin, K. Improving coral-base

paleoclimate reconstructions by replicating 350 years of coral Sr/Ca variations. *Palaeogeography, Palaeoclimatology, Palaeoecology* **373**, 6-24 (2013).

26 Quinn, T. M. *et al.* A multicentury stable isotope record from a New Caledonia coral: Interannual and decadal sea surface temperature variability in the southwest Pacific since 1657 AD. *Paleoceanography* **13**, 412 (1998).

27 Calvo, E. *et al.* Interdecadal climate variability in the Coral Sea since 1708 AD. *Palaeogeography, Palaeoclimatology, Palaeoecology* **248**, 190-201 (2007).

28 Burrows, M. A., Fenner, J. & Haberle, S. G. Humification in northeast Australia: Dating millennial and centennial scale climate variability in the late Holocene. *The Holocene*, Online first, DOI: 10.1177/0959683614551216 (2014).

29 Burrows, M., Fenner, J. & Haberle, S. Testing peat humification analysis in an Australian context: identifying wet shifts in regional climate over the past 4000 years. *Mires and Peat* **14**, 1-19 (2014).

30 Rodysill, J. R. *et al.* A paleolimnological record of rainfall and drought from East Java, Indonesia during the last 1,400 years. *Journal of Paleolimnology* **47**, 1-15 (2012).

31 Griffiths, M. *et al.* Increasing Australian-Indonesian monsoon rainfall linked to early Holocene sea-level rise. *Nat Geosci* **2**, 636-639 (2009).

32 Konecky, B. L. *et al.* Intensification of southwestern Indonesian rainfall over the past millennium. *Geophysical Research Letters* **40**, 386-391 (2013).

33 Rodysill, J. R. *et al.* A severe drought during the last millennium in East Java, Indonesia. *Quaternary Science Reviews* **80**, 102-111 (2013).

34 Hartmann, A. *et al.* Multi-proxy evidence for human-induced deforestation and cultivation from a late Holocene stalagmite from middle Java, Indonesia. *Chem Geol* **357**, 8-17 (2013).

35 Donohoe, A., Marshall, J., Ferreira, D. & Mcgee, D. The relationship between ITCZ location and cross-equatorial atmospheric heat transport: from the seasonal cycle to the last glacial maximum. *Journal of Climate* **26**, 3597-3618 (2013).

36 Laskar, J., Fienga, A., Gastineau, M. & Manche, H. La2010: a new orbital solution for the long-term motion of the Earth. *Astronomy & Astrophysics* **532**, A89 (2011).

37 Bard, E., Raisbeck, G., Yiou, F. & Jouzel, J. Solar irradiance during the last 1200 years based on cosmogenic nuclides. *Tellus B* **52**, 985-992 (2000).

38 Steinhilber, F., Beer, J. & Fröhlich, C. Total solar irradiance during the Holocene. *Geophysical Research Letters* **36**, L19704 (2009).

39 Sigl, M. *et al.* Insights from Antarctica on volcanic forcing during the Common Era. *Nature Climate Change* **4**, 693-697 (2014).

40 Liu, J. *et al.* Centennial variations of the global monsoon precipitation in the last millennium: Results from ECHO-G model. *Journal of Climate* **22**, 2356-2371 (2009).

41 Steinke, S. *et al.* Mid to Late-Holocene Australian-Indonesian summer monsoon variability. *Quaternary Science Reviews* **93**, 142-154 (2014).

42 Jungclaus, J. H. *et al.* Climate and carbon-cycle variability over the last millennium. *Clim Past* **6**, 723-737 (2010).

43 Conroy, J. L., Overpeck, J. T. & Cole, J. E. El Nino/Southern Oscillation and changes in the zonal gradient of tropical Pacific sea surface temperature over the last 1.2 ka. *PAGES news* **18**, 32-34 (2010).

44 Cobb, K. M., Charles, C. D., Cheng, H. & Edwards, R. L. El Nino/Southern Oscillation and

tropical Pacific climate during the last millennium. *Nature* **424**, 271-276 (2003).

45 Conroy, J. L., Overpeck, J. T., Cole, J. E., Shanahan, T. M. & Steinitz-Kannan, M. Holocene changes in eastern tropical Pacific climate inferred from a Galapagos lake sediment record. *Quaternary Science Reviews* **27**, 1166-1180 (2008).

46 Vecchi, G. A. *et al.* Weakening of tropical Pacific atmospheric circulation due to anthropogenic forcing. *Nature* **441**, 73-76 (2006).

47 Lamb, H. The early medieval warm epoch and its sequel. *Palaeogeography, Palaeoclimatology, Palaeoecology* **1**, 13-37 (1965).

48 Trenberth, K. Signal versus noise in the Southern Oscillation. *Mon Weather Rev* **112**, 326-332 (1984).

49 Bretherton, C. S., Widmann, M., Dymnikov, V. P., Wallace, J. M. & Blade, I. The effective number of spatial degrees of freedom of a time-varying field. *Journal of Climate* **12**, 1990-2009 (1999).

50 Box, G. E. P., Jenkins, G. M. & Reinsel, G. C. *Time series analysis: forecasting and control*. Vol. 16 (Holden-day San Francisco, 1976).